PHYSICAL REVIEW B VOLUME 36, NUMBER 6 15 AUGUST 1987-II

Adsorption on narrow-gap semiconductors

H. J. Kreuzer,* D. Neilson, and J. Szymanski†
School of Physics, University of New South Wales, Kensington, New South Wales, 2033, Australia
(Received 19 June 1986)

A modified Anderson-Newns model for chemisorption on narrow-gap semiconductors is set up. We solve it for the case of an n-type degenerate direct-gap system with an adsorbed atom level lying close to the semiconductor Fermi energy. Changes of local density of states, binding energies, and charge transfers are calculated in the presence of an adatom as a function of the band gap and Fermi energy. We argue that since it is the charge transfer that binds the adatom to the crystal, for the purpose of obtaining trends we can replace the surface Green's functions by their bulk counterparts in the above calculation.

I. INTRODUCTION

Adsorption of gases on clean metal and insulator surfaces has been studied extensively over the past two decades with a considerable amount of work also done for reactive gases like O_2 and CO adsorbing on wide-band-gap elemental, II-VI, and III-V compound semiconductors. Similar studies on narrow-band-gap semiconductors seem to be few. The experimental difficulties involved and the kind of interesting phenomena one might encounter have been discussed recently by Spicer *et al.*[1] for HgCdTe. We are only aware of one theoretical paper[2] that calculates chemisorption energies of oxygen on narrow-band-gap semiconductors. It might be appropriate to briefly recapitulate the main features of narrow-band-gap semiconductors that introduce novel aspects into the adsorption of gases.[3] (i) In ternary alloys like $Hg_{1-x}Cd_xTe$ the band gap varies as a function of concentration x between 1.2 eV and -300 meV, being 0 at $x=18\%$. Systematic trends in adsorption characteristics like heat of adsorption, local density of states, charge transfer, etc., should develop as a function of x, as demonstrated in the model calculations presented here. (ii) The bands of narrow-band-gap semiconductors are nonparabolic with considerable s-p mixing away from the center of the Brillouin zone affecting the hopping probabilities onto or from like energy levels of the adsorbing molecule. (iii) Even at low temperature n-type materials can have an electron concentration in the conduction band that is typically of the order of 10^{15} cm^{-3}. Crossing the Fermi energy with the affinity level of the adsorbing molecule as a function of doping and alloying should produce systematic trends in the heat of adsorption and charge transfer. (iv) Upon adsorption new surface states for holes or electrons may develop to either enhance or hinder further adsorption. Surface segregation of one or the other alloy component may also occur. (v) A systematic study of the dynamics of the adsorption and desorption processes will reveal the relative importance of phonons versus electron-hole pairs in mediating the energy transfer between solid and adsorbate.[4] Carrier mobilities towards the surface will determine the efficiency of charge transfer. (vi) Because narrow-band-gap semiconductors are efficient infrared absorbers, photodesorption and photocatalysis via vibrational molecular modes should be promising.[5] This is in addition to the electronic effects widely observed on wide-band-gap semiconductors.[6–8] We hope to elaborate on points (v) and (vi) in a future paper.

None of the above properties of narrow-band-gap semiconductors should produce any surprises for physisorption, as born out by a recent calculation of the Van der Waals interaction of rare gases and hydrogen on some 20 semiconductor surfaces.[9] However, for chemisorption new features should emerge. In this paper we have therefore set up an Anderson-type model to study the equilibrium properties of a molecule adsorbed on a narrow-band-gap semiconductor following similar work by Newns,[10] Edwards and Newns,[11] Einstein and Schrieffer,[12] and Einstein[13] dealing with chemisorption on metals; for a recent review see Einstein, Hertz, and Schrieffer.[14] In the Anderson-Newns model of chemisorption the adsorbing molecule is idealized to a single relevant electronic energy level of energy E_a, while the substrate is described by a single-band tight-binding model with the surface being explicitly introduced[12–14] via the method of Kalkstein and Soven.[15]

In this study we shall concentrate on doped n-type semiconductor material with free carriers in the conduction band at $T=0$, and with an adsorbed atom level E_a lying close to the Fermi energy E_F. Our many-body Green's functions are calculated using the Kane two-band model[16] which describes accurately the free electrons in the conduction band. The only previous attempt to deal with adsorption on narrow-band-gap semiconductor surfaces was by Davison and Huang[2] who used an s-p molecular-orbital model treated in the tight-binding approximation. It is not clear how this approach could be used for the doped semiconductor with free carriers present.

We expect the dominant contribution to the binding of the adatom to the surface to be due to a net transfer of charge between the atom and the surface, so that details of the surface and directionality should not be of greatest importance.[17] In this particular calculation we are mainly interested in systematic trends as a function

 ©1987 The American Physical Society

of the position of the Fermi level relative to the adatom level E_a. The full Kalkstein-Soven method, while tractable, is rather unwieldy in this system because of the large number of orbitals. For these reasons we avoid using the full Kalkstein-Soven formalism here and approximate the surface Green's functions by their bulk counterparts. This means that the trends we see in our results are due to charge transfer effects. Of course should surface states or surface reconstruction be observed then a complete treatment of the surface would be necessary from the outset.

We treat the adatom level E_a as a phenomenological parameter which should be determined experimentally.[14] One cannot identify E_a with the ionization energy of the isolated atom because of the proximity of the ionic cores of the substrate atoms.

In Sec. II we formulate our model by specifying the Hamiltonian for a narrow-band-gap semiconductor interacting with an adatom and calculating the resulting Green's functions. In Sec. III we use these Green's functions to obtain the local density of states, the binding energy of the adsorbed atom, and the charge transfer for a range of Fermi energies, band gaps, and hopping strengths. Section IV contains a brief conclusion.

II. THEORY

In this section we formulate the Anderson-Newns model to calculate the adsorption characteristics of a molecule on a narrow-band-gap semiconductor. We first set up the Hamiltonian in Sec. II A and then calculate the relevant Green's functions in Sec. II B.

A. The Hamiltonian

We split the Hamiltonian for the electrons of the coupled gas-solid system into three parts

$$H = H_a + H_s + V \ . \tag{1}$$

In second quantization the Hamiltonian for the adsorbing molecule reads

$$H_a = \sum_{\sigma=\uparrow,\downarrow} E_a c_{a\sigma}^{\dagger} c_{a\sigma} + U c_{a\uparrow}^{\dagger} c_{a\uparrow} c_{a\downarrow}^{\dagger} c_{a\downarrow} \ , \tag{2}$$

where E_a is the energy of the only participating electron level on the molecule; $c_{a\sigma}^{\dagger}$ creates an electron of spin $\sigma=\uparrow$ or $\downarrow$ bound with an energy E_a to the molecule far from the solid; $c_{a\sigma}$ removes an electron. U is the average strength of the Coulomb repulsion between two electrons in the state a.

The isolated narrow-band-gap semiconductor is treated in the Kane two-band model[16] for which the Hamiltonian reads

$$H_s = \sum_{\lambda,\lambda'\sigma,\sigma',\mathbf{k}} \epsilon_{\lambda\sigma\lambda'\sigma'}(\mathbf{k}) c_{\lambda\sigma}^{\dagger}(\mathbf{k}) c_{\lambda'\sigma'}(\mathbf{k}) \ . \tag{3}$$

Here $\lambda=0,\ldots,3$ labels the two bands with $l=0$ and $l=1$, respectively, the latter with $l_z=0,\pm 1$. The 8×8 matrix $\underline{\epsilon}(\mathbf{k})$ is given by Kane as a function of the wave vector $\mathbf{k}$. In the following we work in a basis in which $\underline{\epsilon}$ is diagonal. It can be generated by a transformation to a new set of creation and annihilation operators

$$d_{n\alpha}(\mathbf{k}) = \sum_{\lambda,\sigma} \langle n\alpha \mid \lambda\sigma \rangle c_{\lambda\sigma}(\mathbf{k}) \tag{4}$$

so that

$$H_s = \sum_{n,\alpha,\mathbf{k}} E_{n\alpha}(\mathbf{k}) d_{n\alpha}^{\dagger}(\mathbf{k}) d_{n\alpha}(\mathbf{k}) \ . \tag{5}$$

Here $n=1,\ldots,4$ enumerates the four twofold degenerate $(\alpha=1,2)$ bands which can be characterized by their symmetry properties at the zone center $\mathbf{k}=0$ as Γ_6, Γ_7, Γ_8^h, and Γ_8^l, where Γ_8^h refers to a band of heavy holes and Γ_8^l to light holes, the latter becoming electrons for a zero-gap semiconductor; see Fig. 1. The above formulation is appropriate for a bulk semiconductor. We postpone a discussion of intrinsic surface states to Secs. II B and III.

We next turn to the interaction V between a molecule and the solid. It is mediated by electron hopping

$$V = \frac{1}{\sqrt{N}} \sum_{\lambda,\sigma,\mathbf{k}} [V_{\lambda\sigma}(\mathbf{k}) c_{\lambda\sigma}^{\dagger}(\mathbf{k}) c_{a\sigma} + V_{\lambda\sigma}^{*}(\mathbf{k}) c_{a\sigma} c_{\lambda\sigma}(\mathbf{k})] \ , \tag{6}$$

where N is the number of elementary cells in the crystal. Rather than attempting to calculate the hopping integrals $V_{\lambda\sigma}(\mathbf{k})$ from first principles, we will treat them as phenomenological parameters that account for the couplings with the various angular momentum states of the semi-

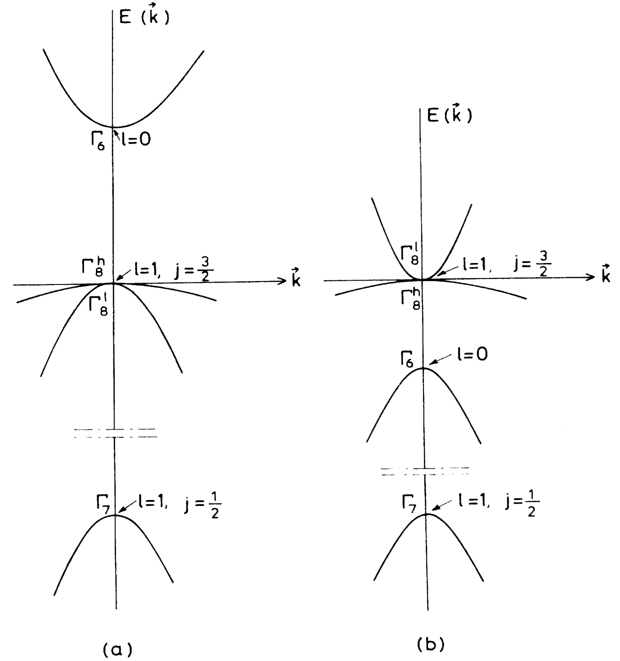

FIG. 1. (a) Configuration of bands for the open-gap semiconductor. The labels l and j refer to the orbital angular moment and total angular momentum at $\mathbf{k}=\mathbf{0}$. Γ_8^h refers to a band of heavy holes and Γ_8^l to light holes. (b) Configuration of bands for the zero-gap semiconductor. Γ_8^l now refers to the electrons.

conductor. We note that (6) does not imply that the state a on the molecule has well-defined l or l_z. The hopping Hamiltonian V is assumed to be diagonal in spin and we also neglect Coulomb repulsion between an electron on the molecule and an electron in the solid. Image charge effects are also omitted. For a discussion of these approximations see, e.g., Einstein *et al.*[14]

B. Green's functions

We now proceed to calculate the various zero-temperature Green's functions. For the isolated molecule described by H_a in (2) we get in the Hartree-Fock approximation

$$G^0_{a\sigma\sigma'}(E,n_{a,-\sigma})=\delta_{\sigma\sigma'}\frac{1}{E-E_a-Un_{a,-\sigma}+i\eta}\ , \tag{7}$$

where $n_{a\sigma}$ is the occupation number of state a with spin σ. For the interacting molecule we get

$$G_{a\sigma\sigma'}(E)=\sum_{\sigma''}G^0_{a\sigma\sigma''}(E,n_{a,-\sigma})[\underline{\Gamma}(E)]^{-1}_{\sigma''\sigma'}\ , \tag{8}$$

where $\underline{\Gamma}(E)$ is a 2×2 matrix in spin space,

$$\Gamma_{\sigma\sigma'}(E)=\left[\delta_{\sigma\sigma'}-\frac{1}{N}\sum_{\lambda,\lambda',\mathbf{k},\mathbf{k}'}V_{\lambda\sigma}(\mathbf{k})G^0_{\lambda\sigma\lambda'\sigma'}(\mathbf{k},\mathbf{k}',E)V_{\lambda'\sigma'}(\mathbf{k}')G^0_{a\sigma'\sigma'}(E,n_{a,-\sigma'})\right]\ . \tag{9}$$

The Green's function for the isolated semiconductor is

$$G^0_{\lambda\sigma\lambda'\sigma'}(\mathbf{k},\mathbf{k}',E)=\sum_{n,\alpha}\langle\lambda'\sigma'\,|\,n\alpha\rangle\langle n\alpha\,|\,\lambda\sigma\rangle G^0_{n\alpha}(\mathbf{k},\mathbf{k}',E)\ , \tag{10}$$

where

$$G^0_{n\alpha}(\mathbf{k},\mathbf{k}',E)=\delta_{\mathbf{k},\mathbf{k}'}[E-E_{n\alpha}(\mathbf{k})+i\eta]^{-1}\ . \tag{11}$$

Similarly we find for the Green's function of the semiconductor interacting with the molecule

$$G_{\lambda\sigma\lambda'\sigma'}(\mathbf{k},\mathbf{k}',E)=G^0_{\lambda\sigma\lambda'\sigma'}(\mathbf{k},\mathbf{k}',E)+\frac{1}{N}\sum_{\substack{\lambda'',\sigma'',\mathbf{k}''\\ \lambda''',\sigma''',\mathbf{k}'''}}G^0_{\lambda\sigma\lambda''\sigma''}(\mathbf{k},\mathbf{k}'',E)V_{\lambda''\sigma''}(\mathbf{k}'')G_{a\sigma''\sigma'''}(E)V_{\lambda'''\sigma'''}(\mathbf{k}''')G_{\lambda'''\sigma'''\lambda'\sigma'}(\mathbf{k}''',\mathbf{k}',E)\ . \tag{12}$$

The change in the density of states caused by the hopping interaction between the molecule and the semiconductor is given by

$$\Delta\rho(E)=\Delta\rho_a(E)+\Delta\rho_s(E)\ . \tag{13}$$

The projection onto the molecule is

$$\Delta\rho_a(E)=-\pi^{-1}\,\mathrm{Im}\left[\sum_\sigma G_{a\sigma\sigma}(E)-G^0_{a\sigma\sigma}(E)\right]\ , \tag{14}$$

where Im means "imaginary part." Observing from (7) that

$$[G^0_{a\sigma\sigma}(E)]^2=-\frac{\partial}{\partial E}G^0_{a\sigma\sigma}(E)\ ,$$

we get

$$\Delta\rho_a(E)=\pi^{-1}\,\mathrm{Im}\left[\frac{1}{N}\sum_{\substack{\lambda,\lambda',\mathbf{k}\\ \sigma,\sigma'}}\left[\frac{\partial}{\partial E}G^0_{a\sigma\sigma}(E)\right]V_{\lambda\sigma}(\mathbf{k})\times G^0_{\lambda\sigma\lambda'\sigma'}(\mathbf{k},\mathbf{k},E)V_{\lambda'\sigma'}(\mathbf{k})\times[\underline{1}-\underline{\Lambda}(E)]^{-1}_{\sigma'\sigma}\right]\ , \tag{15}$$

where $\underline{1}$ is the 2×2 unit matrix and

$$\Lambda_{\sigma\sigma'}(E)=-\frac{1}{N}\sum_{\lambda,\lambda',\mathbf{k}}G^0_{a\sigma\sigma}(E)V_{\lambda\sigma}(\mathbf{k})\times G_{\lambda\sigma\lambda'\sigma'}(\mathbf{k},\mathbf{k},E)V_{\lambda'\sigma'}(\mathbf{k})\ . \tag{16}$$

The equivalent expression for the change of the density of states projected onto the semiconductor is

$$\Delta\rho_s(E)=\pi^{-1}\,\mathrm{Im}\left[\frac{1}{N}\sum_{\substack{\lambda,\lambda',\mathbf{k}\\ \sigma,\sigma'}}\left[\frac{\partial}{\partial E}V_{\lambda\sigma}(\mathbf{k})G^0_{\lambda\sigma\lambda'\sigma'}(\mathbf{k},\mathbf{k},E)\times V_{\lambda'\sigma'}(\mathbf{k})\right]\times[\underline{1}-\underline{\Lambda}(E)]^{-1}_{\sigma'\sigma}G_{a\sigma\sigma}(E)\right]\ , \tag{17}$$

so that (12) can eventually be written

$$\Delta\rho(E)=\pi^{-1}\,\mathrm{Im}\left[\sum_{\sigma,\sigma'}\left[\frac{\partial}{\partial E}\Lambda_{\sigma\sigma'}(E)\right][\underline{1}-\underline{\Lambda}(E)]^{-1}_{\sigma'\sigma}\right]\ . \tag{18}$$

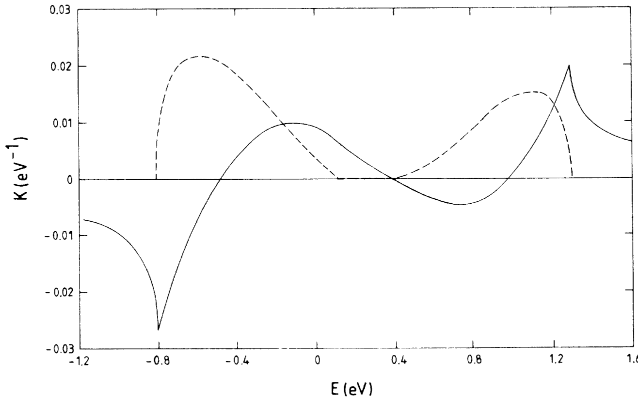

FIG. 2. Typical plot of the Green's function for the isolated semiconductor $\bar{G}(E)=K_1(E)+iK_2(E)$ for energy gap $E_G=0.3$ eV and $E_F=0.3$ eV. Solid line, $K_1(E)$; dashed line, $K_2(E)$.

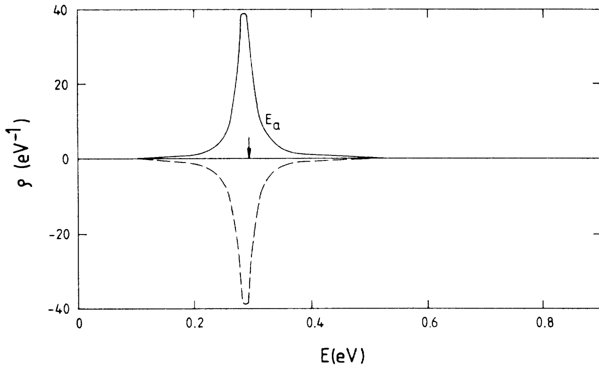

FIG. 3. Density of states for the adatom $\rho_a(E)$ (solid line) and $-\Delta\tilde{\rho}(E)$ (dashed line), defined in (22). The gap energy $E_G=0.3$ eV and the adatom level E_a is located 0.3 eV above the conduction-band edge set at $E=0$. The hopping matrix element $V_0=1.2$ eV and the correlation energy $U=0$.

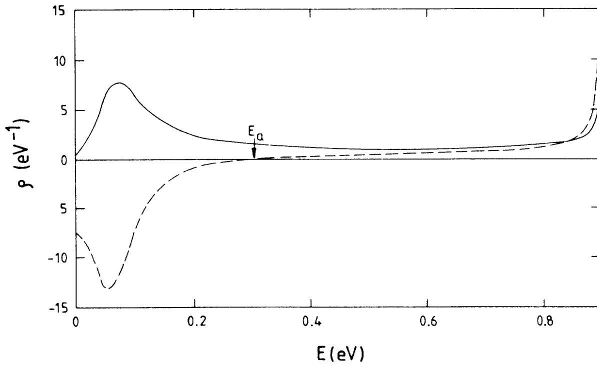

FIG. 4. Same as Fig. 3 except for $V_0=4.8$ eV and $U=0$.

We now assume that the level a on the molecule is an s state so that only the $\lambda=l=0$ substrate states are coupled into it. In this case we can show, using (9), (10), and (A2), that the s component of the semiconductor Green's function $G_{0\sigma0\sigma'}$ is diagonal in spin indices. Equation (16) thus simplifies

$$\Lambda_{\sigma\sigma'}(E)=\delta_{\sigma\sigma'}\frac{1}{N}\sum_{\mathbf{k}} G^0_{a\sigma\sigma}(E)V_{0\sigma}(\mathbf{k}) \times G^a_{0\sigma0\sigma}(\mathbf{k},\mathbf{k},E)V_{0\sigma}(\mathbf{k}) \ . \tag{19}$$

Let us now assume that electron hopping in (6) is restricted to nearest neighbors so that $V_{0\sigma}(\mathbf{k})$ is independent of $\mathbf{k}$. We then get from (18) and (19)

$$\Delta\rho(E)=\pi^{-1}\,\mathrm{Im}\left[\sum_\sigma \frac{\partial}{\partial E}\ln[1-V^2_{0\sigma}G^0_{a\sigma\sigma}(E)\bar{G}_{0\sigma0\sigma}(E)]\right] , \tag{20}$$

where

$$\bar{G}_{0\sigma0\sigma}(E)=\frac{\Omega}{N}\int\frac{d^3k}{(2\pi)^3}G^0_{0\sigma0\sigma}(\mathbf{k},\mathbf{k},E) \ . \tag{21}$$

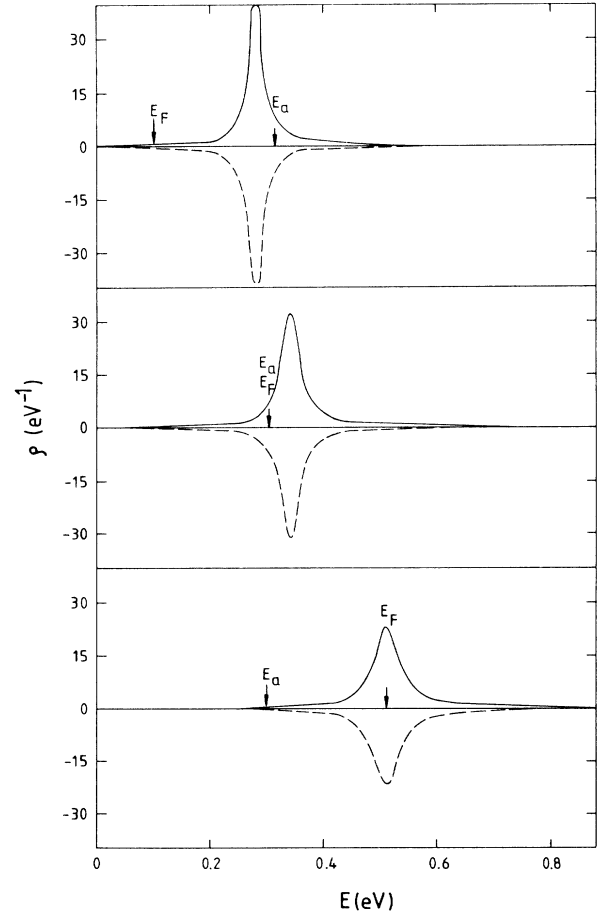

FIG. 5. Same as Fig. 3 except for $V_0=1.2$ eV and $U=1$. Cases (a), (b), and (c) correspond to the Fermi energy $E_F=0.1$, 0.3, and 0.5 eV.

Here Ω is the volume of the crystal. For the fcc lattice $\Omega/N=\frac{1}{2}a_0^3$, where a_0 is the lattice constant. $\bar{G}_{0\sigma0\sigma}(E)$ is derived in the Appendix for the case of the two-band Kane model.

For numerical purposes it is useful to remove the δ-function contribution from $\Delta\rho(E)$ by defining

$$\Delta\tilde{\rho}(E)=\Delta\rho(E)+2\delta(E-E_a)\ , \tag{22}$$

which is given by

$$\Delta\tilde{\rho}(E)=\pi^{-1}\,\mathrm{Im}\left\{\sum_\sigma \frac{\partial}{\partial E}\ln[E-E_a+Un_{a,-\sigma}+i\eta - V_{0\uparrow}^2\bar{G}_{0\uparrow0\uparrow}(E)]\right\}\ . \tag{23}$$

In the absence of magnetic fields $n_{a\sigma}=n_{a-\sigma}$ so that in (18) and (23) the spin sum simply yields a factor of 2. Within the Hartree-Fock approximation, $n_{a\sigma}$ must be calculated self-consistently from

$$n_{a\sigma}=\tfrac{1}{2}\int_{-\infty}^{E_F} dE\,\rho_a(E)\ , \tag{24}$$

where E_F is the Fermi energy and

$$\rho_a(E)=-\pi^{-1}\,\mathrm{Im}\left[\sum_\sigma G_{a\sigma}(E)\right] = -2\pi^{-1}\,\mathrm{Im}\{[E-E_a-Un_{a\uparrow}-V_{0\uparrow}^2\bar{G}_{0\uparrow0\uparrow}(E)]^{-1}\}\ . \tag{25}$$

Lastly we note that the binding energy of the molecule onto the semiconductor is given by

$$E_b=\int_{-\infty}^{E_F} dE\,(E_F-E)\Delta\rho(E)\ . \tag{26}$$

III. RESULTS AND DISCUSSION

In this section we discuss the implications of the theory. We will present numerical examples of the densities of states (23) and (25) and calculate binding energies and charge transfers for various molecule-semiconductor systems. The systems are characterized for the molecule by the electron level E_a, and for the semiconductor by the band parameters and the Fermi energy.

We begin with a discussion of the Green's function (21) of the isolated semiconductor. Its real and imaginary parts are defined by

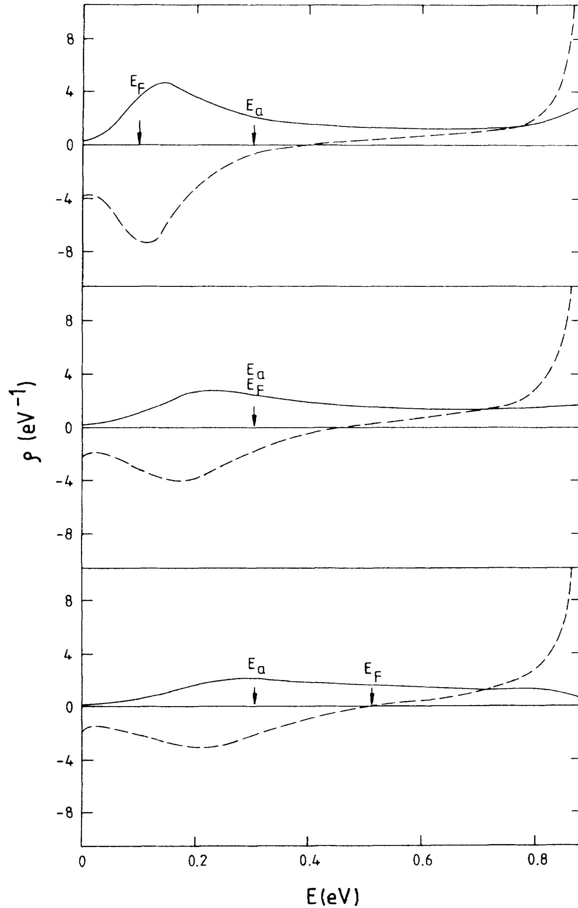

FIG. 6. Same as Fig. 5 except for $V_0=4.8$ eV and $U=1$.

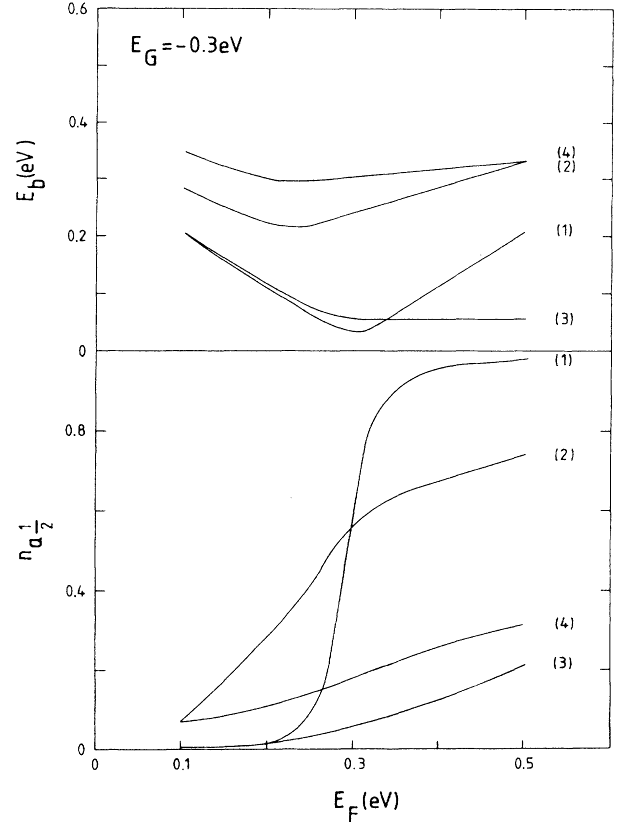

FIG. 7. Binding energy E_b and spin-up occupation number for the adatom state $n_{a/2}$ as a function of the Fermi energy E_F for a fixed gap $E_G=-0.3$ eV. The levels refer to the following cases: (1) $V_0=1.2$ eV, $U=0$; (2) $V_0=4.8$ eV, $U=0$; (3) $V_0=1.2$ eV, $U=1$; (4) $V_0=4.8$ eV, $U=1$.

$$\bar{G}_{0\uparrow0\uparrow}(E)=K_1(E)+iK_2(E)\ . \tag{27}$$

A detailed calculation of this Green's function for narrow-band-gap semiconductors within the Kane band model is given in the Appendix.

Using (27) we can reexpress (23) and (25) for the density of states as follows:

$$\Delta\tilde{\rho}(E)=\frac{2}{\pi}V_0^2\frac{(1-V_0^2K_1')K_2-(E-E_a-V_0^2K_1)K_2'}{(E-E_a-V_0^2K_1)^2+V_0^4K_2^2}\ , \tag{28}$$

$$\rho_a(E)=-\frac{2}{\pi}V_0^2\frac{K_2}{(E-E_a-V_0^2K_1)^2+V_0^4K_2^2}\ , \tag{29}$$

where the prime indicates the derivative with respect to E.

In the present calculation we choose the following values for the parameters associated with the semiconductor substrate:[18] the momentum matrix element $P=7.1$ eV Å, the lattice constant $a_0=6.46$ Å, and the width of both valence and conduction bands $E_B=0.9$ eV.

Figure 2 shows a typical example of $K_1(E)$, in this case for $E_G=0.3$ eV and $E_F=0.3$ eV. Note that the negative values of $K_1(E)$ within the band gap $0<E<0.3$ eV can lead to split-off states just below the conduction band.

In Figs. 3–6 we plot ρ_a and $-\Delta\tilde{\rho}$ for different values of the hopping strength V and the Coulomb repulsion U on the adatom. Note that for clarity it is $-\Delta\tilde{\rho}$ which is plotted. In all these plots the gap energy E_G is fixed at 0.3 eV and the adatom level E_a is located 0.3 eV above the conduction-band edge. We start our energy scale for these figures at the bottom edge of the conduction band, since for the cases presented here $\rho_a(E)$ and $-\Delta\tilde{\rho}(E)$ are very small within the valence band; furthermore the split-off states occur in the gap in these examples.

Figure 3 is our weak hopping case $V_0=1.2$ eV with no Coulomb repulsion $U=0$ between electrons on the adatom. $\rho_a(E)$ exhibits the expected Lorentzian broadened shape and $\Delta\tilde{\rho}(E)=\rho_a(E)$. This implies that the substrate density of states is essentially unmodified.

Figure 4 is the strong hopping case $V_0=4.8$ eV, but with U still kept at 0. The curves are broad and somewhat asymmetric. $\rho_a(E)$ is no longer identical with $\Delta\tilde{\rho}(E)$, and neither curve is centered on the atomic level E_a.

In Figs. 5 and 6 we show the weak and strong hopping cases with the Coulomb repulsion on the adatom switched on: $U=1.0$ eV. As expected for the weak coupling case, when E_F is much larger than E_a [Fig. 5(c)], the $\rho_a(E)$ Lorentzian curve is pushed up toward E_F from its original position at E_a, so that approximately only one electron sits on the adatom. By the same argument, once E_F becomes comparable or smaller than E_a, we would expect the Lorentzian to be centered on E_a and we see this in

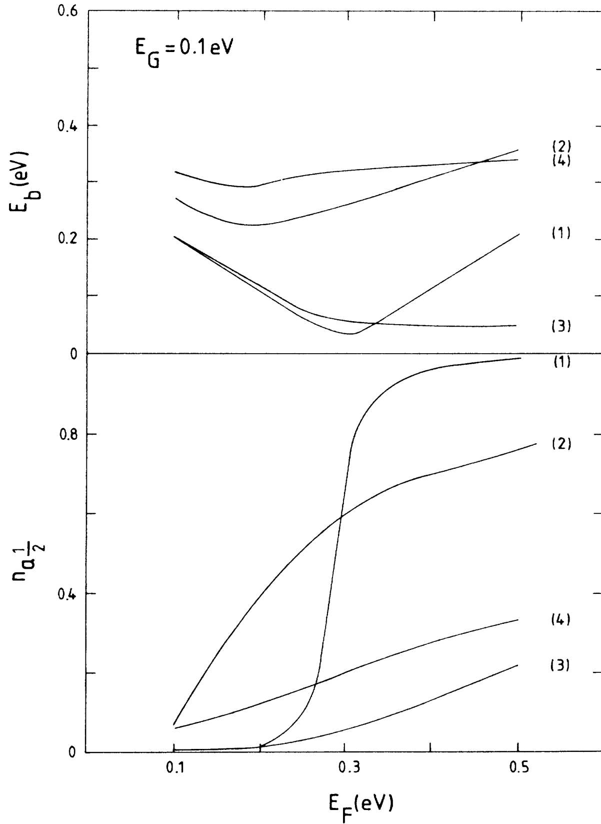

FIG. 8. Same as Fig. 7 for a fixed gap $E_G=0.1$ eV.

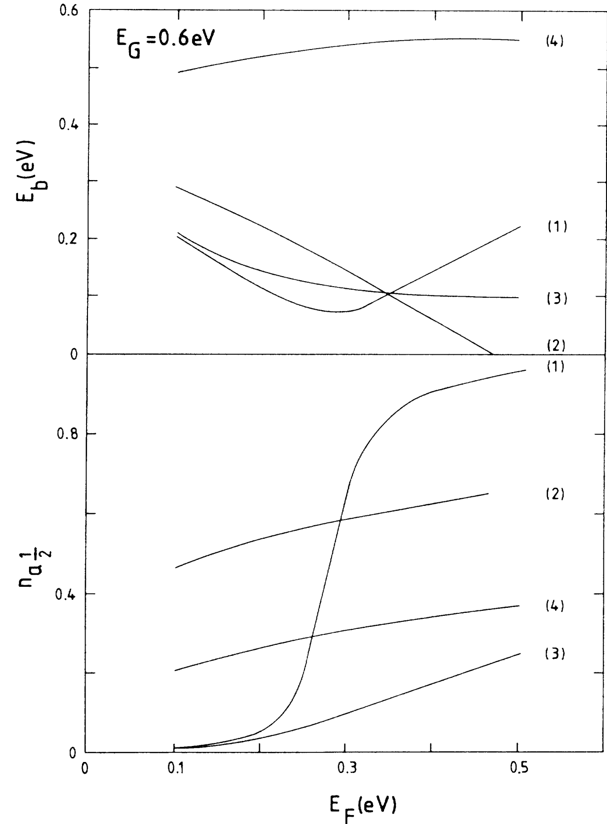

FIG. 9. Same as Fig. 7 for a fixed gap $E_G=0.6$ eV.

Figs. 5(a) and 5(b). For the strong hopping case in Fig. 6, $\rho_a(E)$ is again very broad but we still see the tendency for the peak to shift toward E_F.

In Figs. 7–9 we show the binding energy E_b and the spin-up occupation number for the adatom state $n_{a\uparrow}$ as a function of the Fermi energy for a fixed gap E_G. The adatom state is fixed at $E_a = 0.3$ eV. We note that when $U = 0$, curves (1) and (2), the binding energy E_b exhibits a minimum as E_F passes through E_a. Since in our case the binding is governed mainly by the charge transfer, one should expect the minimum of the binding energy when the charge transfer is smallest. For $U = 1$ eV, curves (3) and (4), electron repulsion on the adatom prevents large charge transfers, and E_b shows no distinct maximum.

In Figs. 10–12 we show E_b and $n_{a\uparrow}$ as a function of the band gap E_G for Fermi energy E_F fixed with respect to the bottom of the conduction band. The adatom state E_a is fixed 0.3 eV above the bottom of the conduction band. In Fig. 10 the Fermi energy E_F is well below the adatom level E_a, and consequently very little charge resides on the adatom in all cases. In Figs. 11 and 12, curve (1) for both E_b and $n_{a\uparrow}$ is almost flat: in this weak hopping case the adatom level is narrow and is not greatly affected by E_G. Contrast this with curve (2), the strong hopping case, where we see both E_b and $n_{a\uparrow}$ dipping sharply as E_G increases. This is due to the change in the effective hopping coupling caused by the relative increase in s-like components in the conduction band as E_G increases. Since we assume an s state for the adatom we only have hopping to the s-like components in the band. Thus this behavior is a direct manifestation of the s-p mixing of the semiconductor bands due to the narrowness of the gap. Finally, curves (3) and (4) (i.e., $U = 1$ eV) in Figs. 11 and 12 show a very weak dependence of $n_{a\uparrow}$ on E_G.

We note in the case of strong coupling $V = 4.8$ eV and for wide gaps we obtain a split-off state in the band gap. These occur at the energy E_0 whenever the denominator in (28) and (29) vanishes, i.e., $E_0 - E_a - V_0^2 K_1(E_0) = 0$ and $K_2(E_0) = 0$. Whether this state is occupied by one or two electrons depends on the strength of the exchange repulsion U between them. For $U = 0$ we get double occupancy. As U increases, E_0 moves up until it becomes energetically favorable for one electron to hop into the conduction band. This switch-over could be observed in real

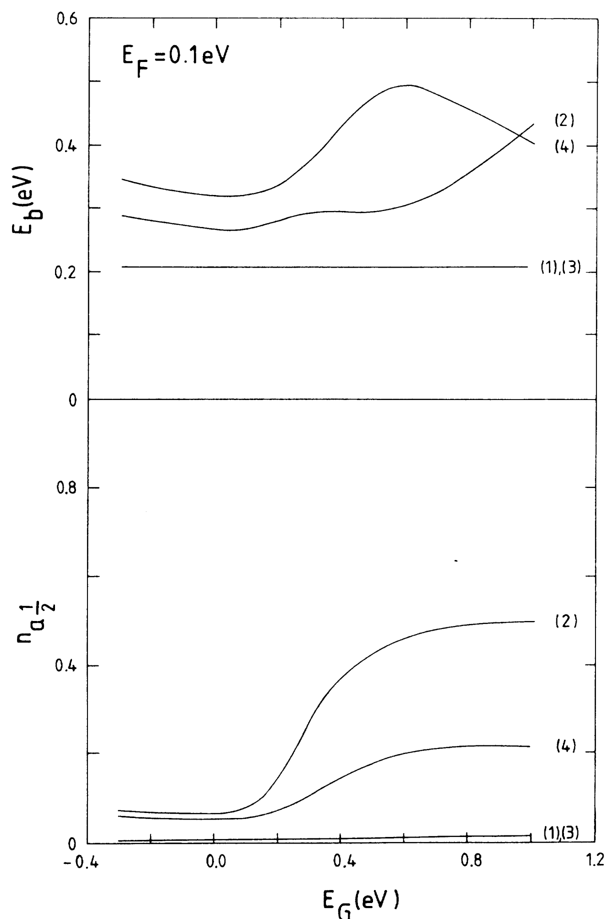

FIG. 10. Binding energy E_b and spin-up occupation number $n_{a\uparrow}$ as a function of the energy gap E_G for a fixed Fermi energy $E_F = 0.1$ eV. The numerical labels refer to the same (V_0, U) combinations as in Fig. 7.

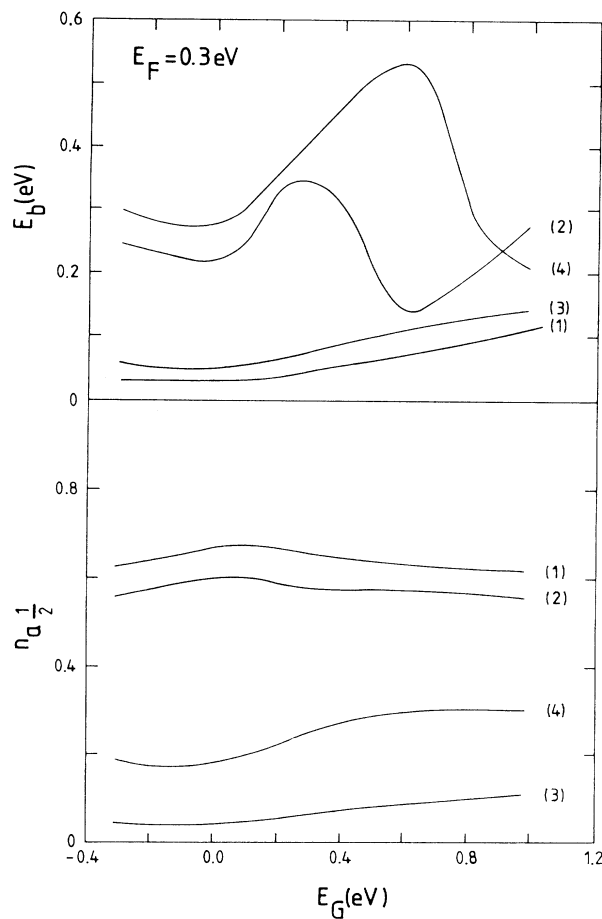

FIG. 11. Same as Fig. 10 for a fixed Fermi energy $E_F = 0.3$ eV.

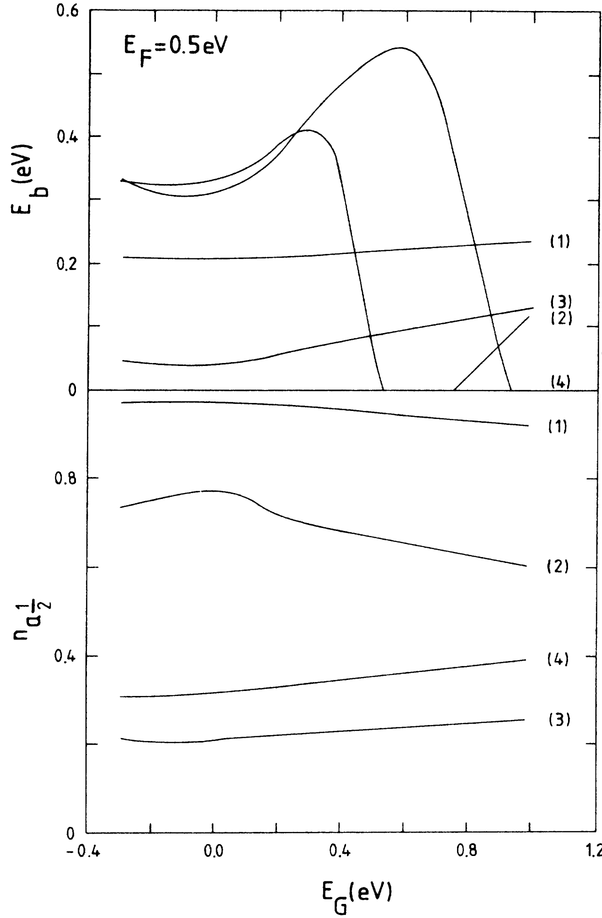

FIG. 12. Same as Fig. 10 for a fixed Fermi energy $E_F=0.5$ eV.

materials as a function of either the Fermi energy (being changed by doping) or the band gap (being changed by alloying). In our particular cases both split-off states for $U=0$ are (of course) doubly occupied while the state for $U=1.0$ eV is singly occupied.

IV. SUMMARY AND OUTLOOK

We have in this paper developed an Anderson-Newns model for chemisorption on narrow-band-gap semiconductors. To describe the semiconductor we use two bands of different symmetries mixed by the $\mathbf{k}\cdot\mathbf{p}$ "interaction." In numerous numerical examples we demonstrated systematic trends in the local density of states, the binding energy, and the charge transfer as a function of Fermi energy (to be varied experimentally by doping) and as a function of the band gap (to be changed by alloying). Split-off states may occur below the conduction band and even below a narrow valence band. Providing the reconstruction of the semiconductor surface does not occur, the corrections to this charge transfer model can be calculated using the Kalkstein-Soven tight-binding formalism. This is a tedious but tractable calculation which we are currently carrying out. Should surface reconstruction be observed then only a complete *ab initio* calculation would suffice.

ACKNOWLEDGMENTS

This work was done while one of us (H.J.K.) was visiting the University of New South Wales. Support through a Special Projects Grant is gratefully acknowledged. Part of this work is also supported through a grant by the Natural Sciences and Engineering Research Council of Canada.

APPENDIX

The purpose of this section is to present a detailed calculation of $\bar{G}_{\lambda\sigma\lambda\sigma}(E)$, which is the only quantity in the theory depending on the band structure. We have, using Eqs. (9), (10), and (21),

$$\bar{G}_{\lambda\sigma\lambda\sigma}(E)=\frac{1}{N}\sum_{\mathbf{k}} G^{0}_{\lambda\sigma\lambda\sigma}(\mathbf{k},\mathbf{k},E)$$
$$=\sum_{n,\alpha}\frac{\Omega/N}{(2\pi)^3}\int d^3k\frac{n_{n\alpha}(\mathbf{k})\,|\langle\lambda\sigma\,|\,n\alpha\rangle|^2}{E-E_{n\alpha}(\mathbf{k})+i\eta}\,, \tag{A1}$$

where Ω is the volume of the crystal, N is the number of elementary cells. For the fcc lattice $\Omega/N=\frac{1}{2}a_0^3$, where a_0 is the lattice constant. The eight wave functions $\langle\mathbf{r}\,|\,\lambda\sigma\rangle$ ($\lambda=0,1,2,3$; $\sigma=\uparrow,\downarrow$) are the periodic parts of the Bloch functions at $\mathbf{k}=\mathbf{0}$ for the conduction and valence bands (s-like and p-type), and are usually denoted by $iS_{\uparrow(\downarrow)}$, $X_{\uparrow(\downarrow)}$, $Y_{\uparrow(\downarrow)}$, $Z_{\uparrow(\downarrow)}$.

To find the wave functions $\langle\mathbf{r}\,|\,n\alpha\rangle$ that diagonalize the crystal Hamiltonian H_s for a narrow-band-gap semiconductor we will use the Kane model. The periodic parts of the Bloch functions $\langle\mathbf{r}\,|\,n\alpha\rangle$ can be written as (see e.g., Ref. 19)

$$u_{n1\mathbf{k}}(\mathbf{r})=\langle\mathbf{r}\,|\,n1\rangle$$
$$=\left[\frac{E_n-E_G}{2E_n-E_G}\right]^{1/2}\left[\left[\frac{E_n}{E_n-E_G}\right]^{1/2}u_2+\tfrac{1}{2}\hat{k}_+u_4+\hat{k}_zu_5+\frac{\sqrt{3}}{2}\hat{k}_-u_6\right]\quad(n=1,2)\,,$$
$$u_{n2\mathbf{k}}=\hat{T}u_{n1\mathbf{k}}\,. \tag{A2}$$

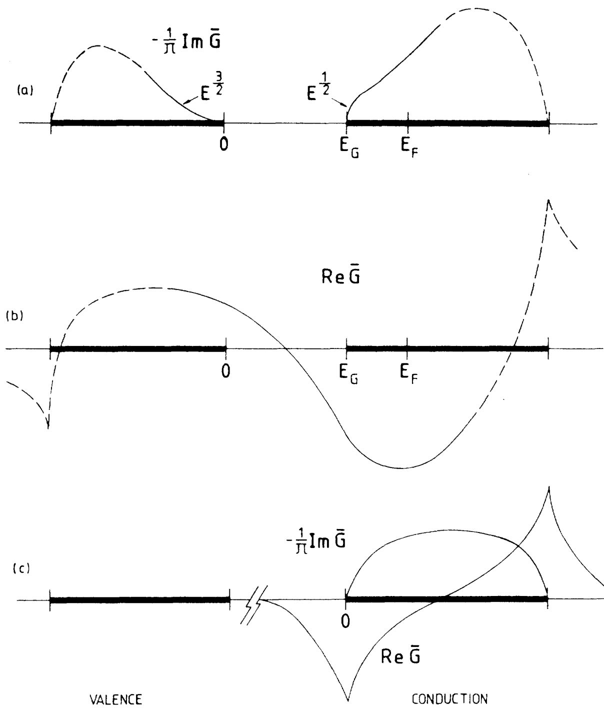

FIG. 13. Schematic plot of imaginary (a) and real (b) parts of the Green's function $\bar{G}$ for a narrow-band-gap semiconductor. The shaded horizontal bars refer to the spread of the bands. Near the band edges $\mathrm{Im}\bar{G}(E)\sim E^{3/2}$ and $E^{1/2}$ as indicated. In the energy range where the Green's functions are shown as dashed lines, their detailed behavior depends on the choice of the lower cutoff for the valence band (see Appendix). (c) Corresponding plot of $\bar{G}(E)$ for a one-band model of a metal.

Here, $\lambda=0$ corresponds to the conduction band, $\lambda=1$ to the valence band. Since in the approximation used here (see below) the two remaining bands (Γ_8^h and Γ_7) do not couple to the s-like wave function, we may omit them. In Eq. (A2), $\mathbf{k}$ is the wave vector and $\hat{k}_\pm=(k_x\pm ik_y)/k$, $\hat{k}_z=k_z/k$. E_G is the energy gap, which is negative for zero-gap materials, E_n $(n=1,2)$ are the two solutions of the quadratic equation

$$E(E-E_G)=\tfrac{2}{3}P^2k^2\ , \tag{A3}$$

where $P=-(i\hbar/m)\langle s\mid \hat{P}_z\mid z\rangle$ characterizes the s-p interband "interaction." u_1 to u_6 are the s-like and p-like Bloch amplitudes at $\mathbf{k}=0$ in the total angular momentum representation

$$u_2=iS_\uparrow,\quad u_1=\hat{T}u_2\ ,$$
$$u_5=\left[\frac{2}{3}\right]^{1/2}Z_\uparrow-\frac{1}{\sqrt{6}}(X+iY)_\downarrow,\quad u_4=\hat{T}u_5\ , \tag{A4}$$
$$u_6=\frac{1}{\sqrt{2}}(X+iY)_\uparrow,\quad u_3=\hat{T}u_6\ .$$

The operator $\hat{T}$ is given by

$$\hat{T}=\hat{R}\,\hat{I}\equiv\begin{bmatrix}0 & 1\\ -1 & 0\end{bmatrix}\hat{K}\,\hat{I}\ , \tag{A5}$$

where $\hat{I}$ is the space-inversion operator, $\hat{R}$ is the time-reversal operator, and $\hat{K}$ is the complex-conjugate operator.

In obtaining (A2) and (A3) two approximations have been made. First, the spin-orbit splitting Δ (the energy distance between Γ_8 and Γ_7 bands—see Fig. 1) is large, and second the "influence" of all other bands on the conduction and valence bands is neglected.

We now proceed with the calculation of $\bar{G}_{\lambda\sigma\lambda\sigma}(E)$ [Eq. (A1)]. For symmetry reasons only two functions are independent: $\lambda=0$ (S), $\sigma=\uparrow$ and $\lambda=1$ (X), $\sigma=\uparrow$. We need to calculate only the former. Using (A2) and (A4), we have

$$|\langle 0\uparrow|n\alpha\rangle|^2=|\langle u_2\,|u_{n\alpha\mathbf{k}}\rangle|^2$$
$$=\frac{E_n(k)}{2E_n(\mathbf{k})-E_G}\quad(n=1,2)\ . \tag{A6}$$

At $T=0$ and for n-type degenerate material (A1) then becomes

$$K\equiv\bar{G}_{0\uparrow0\uparrow}(E)=\frac{\Omega/N}{(2\pi)^3}4\pi\int_0^{k_F}k^2dk\frac{E_c/(2E_c-E_G)}{E-E_c+i\eta}$$
$$+\int_0^{k_B}k^2dkf(k)\frac{E_v/(2E_v-E_G)}{E-E_v+i\eta}\ , \tag{A7}$$

where k_F is the Fermi energy and k_B is the boundary at the Brillouin zone (Fig. 13).

The integral over the conduction band is well defined, since $E_F\sim E_G$. However, the spectrum for $E_v(\mathbf{k})$ given by Eq. (A3) is unrealistic for $E_v\gg E_G$. We introduce a cutoff factor $f(k)$ which forces the width of the conduction band to be E_B,

$$f(k)=[(E_v(k)-E_v(0)+E_B)/E_B]^{1/2}\ . \tag{A8}$$

This procedure does not affect the imaginary part of $K(E)$ in the conduction band, but the real part of $K(E)$ is changed by an amount which is approximately constant provided that E_B is large enough.

---

*Permanent address: Department of Physics, Dalhousie University, Halifax, N.S., Canada B3H 3J5.

†Present address: Telecom Australia Research Laboratories, 770 Blackburn Road, Clayton North 3168, Australia.

[1] W. E. Spicer, J. A. Silverman, P. Morgan, I. Lindan, and J. A. Wilson, J. Vac. Sci. Technol. **21**, 149 (1982).

[2] S. G. Davison and Y. S. Huang, Solid State Commun. **15**, 863 (1974).

[3] See, e.g., *Handbook of Semiconductors*, or the articles by G. Nimtz, B. Schlicht, and R. Dornhaus, in Vol. 98 of *Springer*

Tracts in Modern Physics (Springer, Berlin, 1983).
[4]For a related study on wide-band-gap semiconductors see M. Wautelet, Surf. Sci. **133**, L437 (1983).
[5]Infrared photodesorption on metals and insulators has been reviewed by T. J. Chuang, Surf. Sci. Rep. **3**, 1 (1983).
[6]Th. Wolkenstein, Prog. Surf. Sci. **6**, 213 (1975).
[7]D. Lichtman and Y. Shapira, CRC Crit. Rev. Solid State Mater. Sci. **8**, 93 (1973).
[8]T. Nakayama, Surf. Sci. **133**, 101 (1983).
[9]K. Nath, Z. W. Gortel, and H. J. Kreuzer, Surf. Sci. (to be published).
[10]D. M. Newns, Phys. Rev. **178**, 1123 (1969); Phys. Lett. **33A**, 43 (1970).
[11]D. M. Edwards and D. M. Newns, Phys. Lett. **24A**, 236 (1967).
[12]T. L. Einstein and J. R. Schrieffer, Phys. Rev. B **7**, 3629 (1973).
[13]T. L. Einstein, Phys. Rev. B **12**, 1262 (1975).
[14]T. L. Einstein, J. A. Hertz, and J. R. Schrieffer, in *Theory of Chemisorption*, Vol. 19 of *Topics in Current Physics*, edited by J. R. Smith (Springer, Berlin, 1980).
[15]D. Kalkstein and P. Soven, Surf. Sci. **26**, 85 (1971).
[16]E. O. Kane, J. Phys. Chem. Solids **1**, 249 (1957).
[17]M. Schmeits, A. Mazur, and J. Pollmann, Solid State Commun. **40**, 1081 (1981).
[18]N. B. Brandt, O. N. Belousova, L. A. Bovina, V. I. Stafeer, and Y. G. Ponomarev, Zh. Eksp. Teor. Fiz. **66**, 330 (1974) [Sov. Phys.—JETP **39**, 157 (1974)].
[19]M. A. Makhtiev and T. G. Ismailov, Phys. Status Solidi B **99**, 507 (1980).